Journal of Power Sources 247 (2014) 354–359

Contents lists available at ScienceDirect

Journal of Power Sources

journal homepage: www.elsevier.com/locate/jpowsour

Performance degradation studies on an poly 2,5-benzimidazole high-temperature proton exchange membrane fuel cell using an accelerated degradation technique

Guo-Bin Jung [a], Hsin-Hung Chen [b], Wei-Mon Yan [c, *]

[a] Department of Mechanical Engineering, Fuel Cell Center, Yuan Ze University, Taoyuan 320, Taiwan
[b] Department of Mechatronic Engineering, Huafan University, Taipei 223, Taiwan
[c] Department of Energy and Refrigerating Air Conditioning Engineering, National Taipei University of Technology, Taipei 106, Taiwan

HIGHLIGHTS

- Degradation of fuel cell is studied by accelerated degradation techniques.
- Characterizations are analyzed by AC impedance, CV, and TEM.
- Decline in performance is due to corrosion and thinning of catalyst layer.

ARTICLE INFO

Article history:
Received 4 May 2013
Received in revised form
26 August 2013
Accepted 27 August 2013
Available online 6 September 2013

Keywords:
Performance degradation
ABPBI-based high temperature PEMFC
Accelerated degradation technique
Membrane electrode assemblies (MEAs)

ABSTRACT

In this work, the performance degradation of a poly 2,5-benzimidazole (ABPBI) based high-temperature proton exchange membrane fuel cell (HT-PEMFC) was examined using an accelerated degradation technique (ADT). Experiments using an ADT with 30 min intervals were performed by applying 1.5 V to a membrane electrode assembly (MEA) with hydrogen and nitrogen feeding to the anode and cathode, respectively, to simulate the high voltage generated during fuel cell shutdown and restart. The characterization of the MEAs was performed using in-situ and ex-situ electrochemical methods, such as polarization curves, AC impedance, and cyclic voltammetry (CV), and TEM imaging before and after the ADT experiments. The measured results demonstrated that the ADT testing could be used to dramatically reduce the duration of the degradation. The current output at 0.4 V decreased by 48% after performing ADT testing for 30 min. From the AC impedance, CV and RTGA measurements, the decline in cell performance was found to be primarily due to corrosion and thinning of the catalyst layer (or carbon support) during the first 30 min, leading to the dissolution and agglomeration of the platinum catalyst.
© 2013 Elsevier B.V. All rights reserved.

1. Introduction

A large number of studies and extensive discussion have been performed on the development of a high-temperature proton exchange membrane fuel cell (HT-PEMFC) that operates in the temperature range of 120–200 °C. This type of fuel cell has been proposed to enhance the reaction kinetics and depress the electrode poisoning that occurs in the Nafion-based low-temperature PEMFC (LT-PEMFC) [1]. An HT-PEMFC actually allows higher tolerance to fuel impurities and easier fuel cell cooling, thus improving the resistance of catalysts to pollutants and heat recovery [2–4]. The studies on the HT-PEMFCs based on proton exchange membrane (PEM), such as phosphoric-acid-doped PBI (poly-benzimidazole) membranes with inorganic dopants, with an emphasis on the membrane conductivity (with different humidified test environments of 5–100% RH) have been reported in the literature [5–8]. Regarding the fuel cell performance, many researchers [9–13] have devoted their studies to the effects of the operating conditions on the performance of HT-PEMFC with dry hydrogen and air for the anode and cathode, respectively. However, using humidified hydrogen from reformate and humidified air directly from the atmosphere are more practical under real HT-PEMFC operational situations. For example, the operational durability of a commercial Celtec®-P1000 MEA (BASF, composed of PBI membrane) at 180 °C and 1 bar absolute pressure was demonstrated using realistic

* Corresponding author. Tel.: +886 939259149; fax: +886 2 27314919.
E-mail addresses: wmyan1234@ntut.edu.tw, wmyan@mail.nutn.edu.tw (W.-M. Yan).

0378-7753/$ – see front matter © 2013 Elsevier B.V. All rights reserved.
http://dx.doi.org/10.1016/j.jpowsour.2013.08.112

Nomenclature

A	current
ADT	accelerated degradation technique
I	current density, A cm^{-2}
P	power density, W cm^{-2}
Q	fuel flow rate, sccm
R	resistance
T	temperature, °C
t	time, min
V	voltage
Subscript	
a	anode
c	cathode

reformate (60% H_2, 5 ppm H_2S, 17% CO_2, 2% CO, and 21% H_2O) for over 3000 h with a degradation rate of 20 μV h^{-1} [14]. Other PEM of the PBI family, such as the simpler poly(2,5-benzimidazole) (ABPBI), can be prepared at a lower cost. Further, ABPBI membranes can be fabricated from different acidic solvents, creating the possibility of synthesizing a super-molecular structure with improved water and phosphoric acid uptakes and good mechanical strength compared to PBI [15]. Hence, an ABPBI membrane was selected as the PEM of the present fuel cell study.

Recently, detailed durability tests of HT-PEMFC have been reported [16–23]. Based on the Celtec®-P1000 MEA, Schmidt [23] reported a daily startup–shutdown cycling test (12 h of operation at 160 °C, followed by 12 h of shutdown). After a period of 6500 h with 260 cycles under mild conditions (160 °C and H_2), a performance loss of ca. 11 μV h^{-1} was observed. Long-term power generation tests were conducted for periods of up to 17,860 h, and the results indicated that growth of the Pt catalyst particles occurred during operation, in addition to oxidation of the carbon support [18]. Although a long-term (from several-hundred to ten-thousand hours) steady-state test can reveal the lifespan of fuel cells, the associated costs in labor and time render such tests impractical. Consequently, to reduce the research costs and the testing time, accelerated degradation techniques (ADTs) have been developed for LT-PEMFCs. For example, during fuel cell operation, membrane and catalyst aging can be accelerated by introducing variations in the humidity and the fuel cell temperature [24,25]. Operating fuel cells under continuous start/stop, various (high/low) voltages, or even under abnormally high voltage can be used to simulate the voltage generated at the electrode–electrolyte interface during fuel cell start–stop operation [26]. Due to its importance, the deterioration of the cell performance of LT-PEMFCs has been examined in detail by use of the accelerated degradation techniques (ADTs) [24–29].

Except for the temperature of operation, the operational conditions for LT-PEMFCs and HT-PEMFCs, such as continuous start/stop and humidified hydrogen and humidified air inlet, are quite similar. Abnormal operating conditions, such as the air/fuel boundary created during the shut-down/start-up process at the anode, are well known to increase the cathodic potential to a level higher than the open circuit voltage [30–32]. Therefore, an abnormal voltage is likely generated at the electrode–electrolyte interface of HT-PEMFCs as well as those of LT-PEMFCs. Based on a literature survey, there have been very few reports on the mechanism underlying the deterioration of PBI- or ABPBI-based HT-PEMFCs using ADTs. This lack of understanding of the degradation mechanism motivates the present study. In the present study, the degradation mechanism of an ABPBI-based HT-PEMFC was examined by measuring the polarization curve, catalyst electrochemical reaction area, and AC impedance at various stages of a 1.5 V ADT test. The test progressed in five stages, with each stage lasting 30 min.

2. Materials and methods

2.1. Preparation of H_3PO_4-doped ABPBI membrane as the PEM

Commercial ABPBI membranes (Fumatech, Germany) doped with 85 wt. % H_3PO_4 were prepared. The thickness and size of the ABPBI membranes were 45 μm and 30 × 30 mm^2, respectively. The ABPBI membranes were immersed in 85 wt. % H_3PO_4 at 90 °C for 9 h.

2.2. Preparation of the membrane electrode assemblies and the HT-PEMFC

In this work, the 40 wt.% Pt/C (carbon supported platinum) from E-TEK, fumion® A ABPBI powder from Fumatech, Lithium chloride (LiCl, Alfa Aesar), and *N*-methylpyrrolidone (NMP, Fluka Chemical Co.) were used for the preparation of the catalyst ink. LiCl was used as a stabilizer of the ABPBI/NMP solution. The ABPBI/NMP/LiCl solutions with a ratio of 1:7:2 were prepared by mixing the ABPBI powder with NMP and LiCl. The mixture was then maintained at 120 °C in a nitrogen (N_2) atmosphere for 24 h. Prior to the catalyst loading, the homogenous solution was allowed to cool to 60 °C. The catalyst loading of 0.75 mg Pt cm^{-2} was used for both the anode and the cathode in the present study. To obtain the thoroughly mixed catalyst ink, the prepared ABPBI/NMP/LiCl solutions with catalyst were mixed in an ultrasonic water-bath for at least 5 h. The resulting homogenous catalyst ink was then carefully coated onto a microporous layer (SGL, 10BC) with an active area of 5 cm^2 and dried at 120 °C in a conventional oven to remove the solvent NMP. The carbon cloths coated with the targeted catalyst loading were immersed in deionized water for 24 h to remove LiCl to obtain the anode and the cathode in this study. The as-prepared H_3PO_4-doped ABPBI membranes (Section 2.1) were then sandwiched between the cathode and the anode to produce the membrane electrode assemblies (MEAs) used for further characterization. A homemade fuel cell was used to evaluate the MEA performance. The fuel cell was composed of a pair of graphite bipolar plates, machined with serpentine flow fields, and two brass end plates for holding the bipolar plates in place. Rod heaters were inserted into the end plates to control the cell temperature. The assembled MEA was protected between two 200 μm gaskets (Teflon sheet SD-2000) prior to being fixed into the center of the fuel cell. The procedure described above resulted in an HT-PEMFC for further investigation, and a detailed description of the procedure is available in the publication of related work [9].

2.3. Accelerated degradation technique (ADT)

During start-up and shutdown conditions, air is always used to purge the residual H_2 in the anode side, and therefore a high voltage (e.g., up to 1.5 V) would be generated at the electrolyte–cathode interface. To simulate the effects of the high voltage generated on the degradation of HT-PEMFC, the accelerated degradation technique (ADT) with the application of an external high voltage (1.5 V) to the HT-PEMFC (or MEA) through an external power supply was performed in this work. In the experiment, the 1.5 V is maintained at an extended time period of 30–150 min (instead of a duration of several seconds every start-up/shutdown) to illustrate its impact on the MEA. In the present study, five stages were performed for the ADT testing, with each stage lasting 30 min.

During the ADT testing, gaseous H_2 was supplied to the anode and N_2 to the cathode of the HT-PEMFC at the same flow rate of 100 sccm with 100% humidity, and the fuel cell temperature was maintained at 160 °C. At the start and end of each stage, the performance degradation of the HT-PEMFC was evaluated using polarization curve, AC impedance and electrochemical tests (CV and LSV). In addition, a real-time gas analyzer (RTGA) was used to analyze the composition of gas released from the cathode.

2.4. Fuel cell test and electrochemical evaluations

To understand the characteristics of the MEA degradation after ADT testing, the polarization measurement and the electrochemical characterizations of AC impedance, cyclic voltammetry (CV), and the linear sweep voltammetry (LSV) were performed in this work. The polarization curve of the HT-PEMFC was measured using an FC 5100 fuel cell testing system (CHINO Corporation, Japan). As for the electrochemical evaluations of the AC impedance, cyclic voltammetry (CV) and the linear sweep voltammetry (LSV), a CHI 1127A (CH Instruments, Inc., USA) was used in the present study.

The operational conditions of the polarization measurement were 160 °C, R.H. 0%, and 100 sccm for both the hydrogen and oxygen flow rates. No back pressure was used. The operational conditions for the AC impedance measurement were exactly the same as those for the polarization measurement. Three current densities, 0.1, 0.2, and 0.5 A cm^{-2}, were used during the AC impedance measurements. The frequency scanning range was 10 kHz to 0.1 Hz, and the amplitude was 5% of the current densities loading. The following operational conditions were used for the CV and LSV analyses. The gas fed to the anode was 100 sccm hydrogen humidified with R.H. 100%. The anode played two roles as the counter electrode and the reference electrode. Humidified nitrogen with R.H. 100% was supplied at the cathode (working electrode). The scanning speed of the LSV method was 1 mV s^{-1}, the sampling speed was 1 mV $point^{-1}$, and the scanning range was 0–1.23 V. The scanning speed of the CV method was 50 mV s^{-1}, the sampling speed was 1 mV $point^{-1}$, and the scanning range was 0–0.8 V. Table 1 summarizes the operating parameters and the gas compositions used during the fuel cell tests and the electrochemical evaluations.

3. Results and discussion

The cell performance of the HT-PEMFC was investigated at various operating temperatures under the non-humidification condition, as indicated in Fig. 1. The cell performance was observed to increase significantly when the cell temperature increased from 150 °C to 170 °C; the cell performance then only gradually increases with the further increase in the cell temperature (up to 180 °C) in the range of the present work. The characteristics of proton-conducting ABPBI material are well-known to be greatly affected by the operating temperature. Higher temperature

Table 1
Summary of the operating parameters and the gas compositions used during the fuel cell test and the electrochemical evaluations.

	I–V curve	AC impedance	CV	LSV
Anode/cathode gas type	H_2/O_2	H_2/O_2	H_2/N_2	H_2/N_2
Anode/cathode gas flow rate (sccm)	100/100	100/100	100/100	100/100
Fuel cell temperature	150–180 °C	160 °C	160 °C	160 °C
Scan frequency		0.1–10,000 Hz	50 mV s^{-1}	1 mV s^{-1}
Scope range (scan range)	0.3–0.9 V	100 mA cm^{-2} 200 mA cm^{-2} 500 mA cm^{-2}	0–0.8 V	0–1.23 V

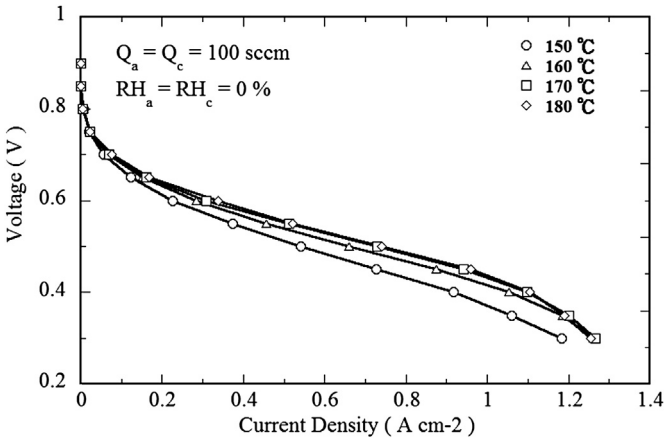

Fig. 1. Effects of the cell temperature on the *I–V* curves of a high-temperature PEM fuel cell.

accelerates the electrochemical reaction and yields better conductivity. However, the higher temperature also presents the possibility of polyphosphoric acid formation and hence decreases the conductivity of the membrane. The counteracting effect of the cell temperature on the high-temperature PEM fuel cell performance may exist at some temperature (e.g., a temperature of approximately 190–200 °C).

Fig. 2 presents the cell performance curves of *I–V* and *I–P* at various stages of the ADT testing. It is clear in Fig. 2(a) that the cell performance was degraded at each aging increment. The

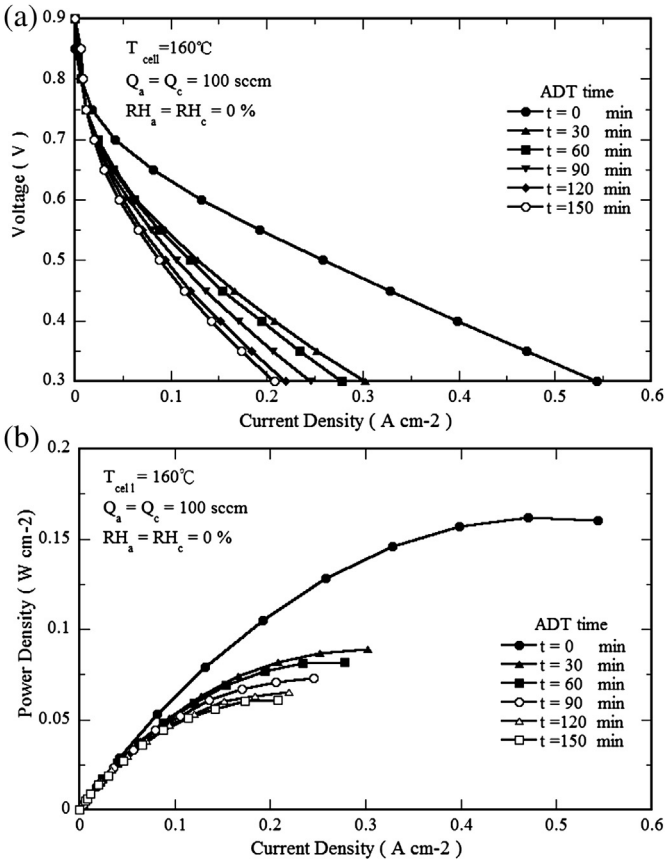

Fig. 2. The cell performance curves at various stages of the ADT testing. (a) *I–V* curves and (b) *I–P* curves.

corresponding current density (A cm^{-2}) of the fuel cell measured at 0.4 V for each stage of the ADT test was 0.40 A cm^{-2} (initial), 0.21 A cm^{-2} (30 min), 0.19 A cm^{-2} (60 min), 0.17 A cm^{-2} (90 min), 0.15 A cm^{-2} (120 min), and 0.14 A cm^{-2} (150 min). Apparently, the cell performance of the HT-PEM fuel cell was dramatically affected at stage 1. Careful inspection of Fig. 2(b) reveals that the maximum power densities at the beginning and at the end of aging process were 0.15 W cm^{-2} and 0.05 W cm^{-2}, respectively. In addition, the slope of the ohmic polarization zone increases with the ADT times. The steeper slope of the ohmic polarization zone indicates the larger total resistances of ion resistance, electrode resistance, and interfacial contact resistance.

The AC impedance diagrams of the HT-PEM fuel cell under different ADT times with various current densities are shown in Fig. 3, which clearly indicates that the charge transfer resistances decreased with increasing current densities. The activation overpotential is the driving force of charge transfer. Therefore, a higher charge transfer resistance is noted for the case with a lower current density ($I = 0.1$ A cm^{-2}) in Fig. 3(a) owing to the lower driving force [33]. Careful inspection of Fig. 3(a) reveals that the cathode polarization losses (R_c, low frequency) at various stages of ADT testing were 3.3 Ω cm^2 (initial), 4.2 Ω cm^2 (30 min), 4.8 Ω cm^2 (60 min), 5.0 Ω cm^2 (90 min), 5.5 Ω cm^2 (120 min), and 5.8 Ω cm^2 (150 min). These losses indicate that the cathode polarization losses progressively increased with the ADT times, which led to a decrease in cell performance, as shown in Fig. 2. This loss mechanism is supported by the fact that the accelerated degradation process literally degraded the catalyst and ionomer, which in turn, caused the larger diameter of the semi-circle. The Nyquist plots for the cell loadings of 0.2 A cm^{-2} and 0.5 A cm^{-2} are presented in Fig. 3(b) and (c), respectively. Comparison of the corresponding curves in Fig. 3(a)–(c) indicated that with the increase of current densities, the charge transfer resistances decreased. This inverse relationship is due to the higher current density leading to a higher driving force.

The linear sweep voltammetry (LSV) and the cyclic voltammetry (CV) of the HT-PEM fuel cell at various stages of the ADT testing are presented in Fig. 4(a) and (b), respectively. The LSV represents the changes in the H_2 permeation rate through the ABPBI membrane. Fig. 4(a) indicates that the measured curves are almost the same during the ADT duration. This similarity means that the H_2 penetration through the membrane is negligible for the ADT duration. Therefore, the ADT test performed by applying 1.5 V does not damage the membrane of the MEA. This lack of damage agrees with the AC impedance measurements shown in

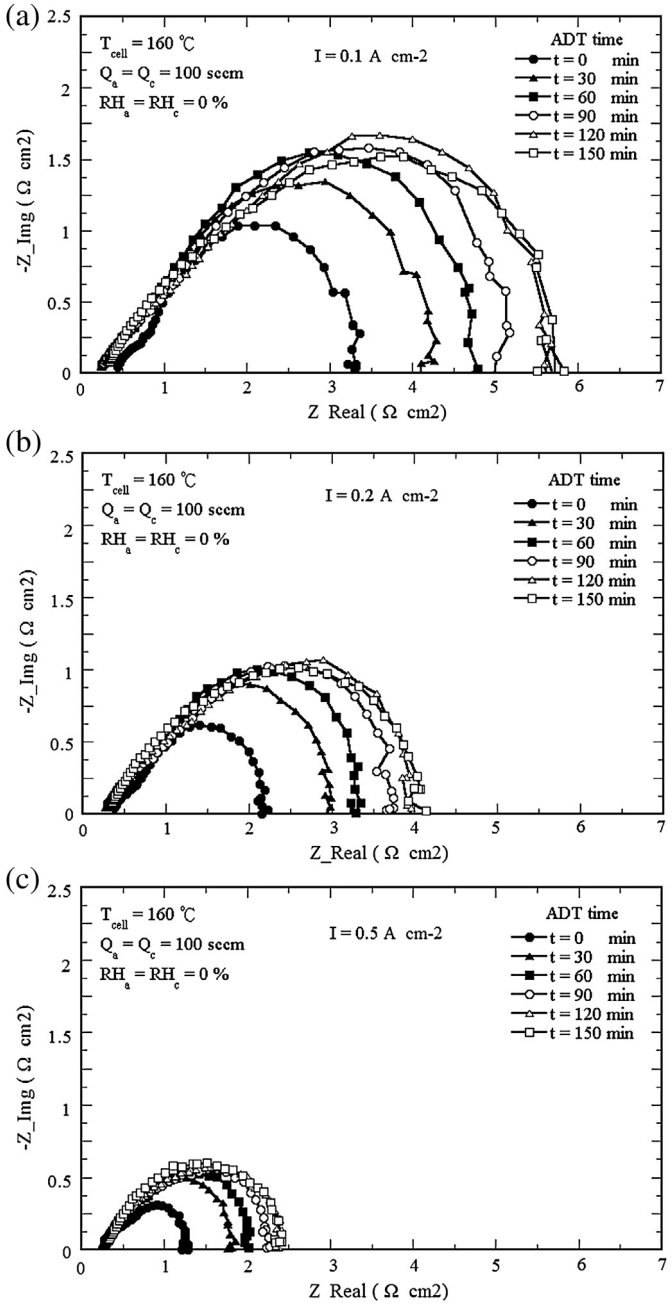

Fig. 3. The AC impedance diagram before and after the ADT testing. (a) $I = 0.1$ A cm^{-2}, (b) $I = 0.2$ A cm^{-2}, and (c) $I = 0.5$ A cm^{-2}.

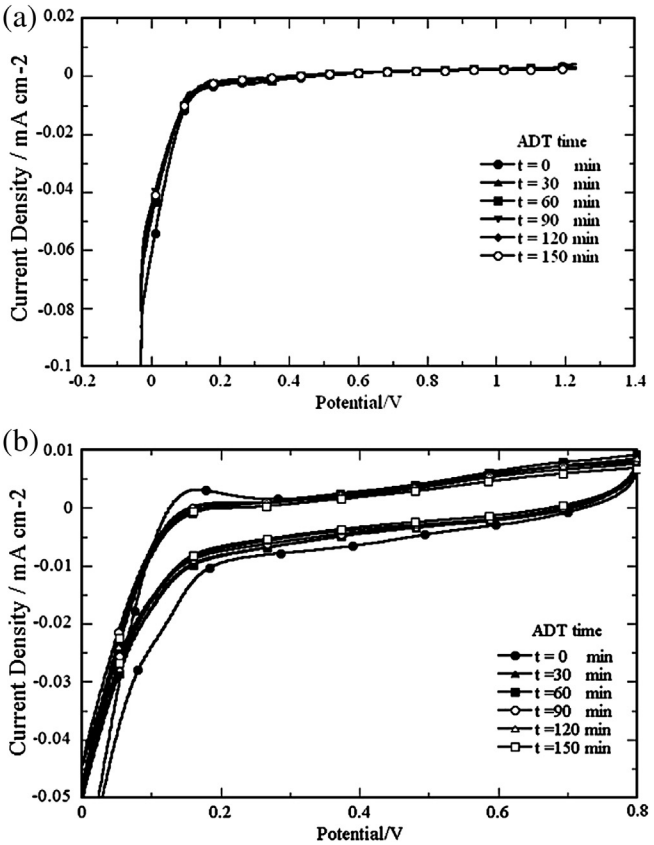

Fig. 4. (a) Linear sweep voltammogram and (b) cyclic voltammogram of the HT-PEM fuel cell at various ADT stages.

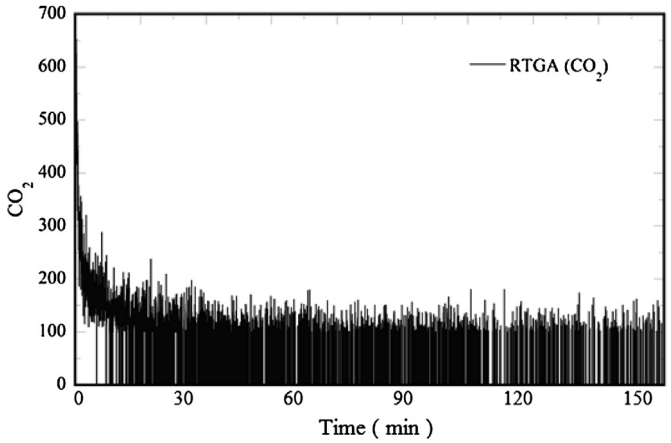

Fig. 5. Real-time gas analysis at the cathode exit during the ADT testing.

Fig. 3, where the ohmic resistance does not change significantly at high frequencies. Therefore, the decline in the cell performance resulting from the 1.5 V ADT test could be due to aging of the cathode catalyst, and not due to damage of the electrolyte membrane.

The electrochemical reaction area in Fig. 4(b) represents the gas adsorption ability of the electrode catalyst. The larger the area is, the higher is the gas adsorption ability of the electrode catalyst. The electrochemical reaction area clearly decreased with an increase in the ADT time. Careful inspection of Fig. 4(b) reveals that the electrochemical reaction area decreases rapidly during the first 30 min of ADT test and then slowly decreases thereafter. As explained in a related work [26], the carbon within the catalyst layer corrodes within 30 min of applying the external high voltage, resulting in dissolution and agglomeration of the platinum within the catalyst layer. This agglomeration raises the ohmic resistance of the HT-PEM fuel cell and reduces the cell performance. The performance reduction was due to either: 1) the dissolution and agglomeration of platinum after 30 min of the ADT test or 2) the corrosion of the carbon support. This feature can be examined further using TEM imaging and will be discussed later.

During the ADT testing, the carbon support in the catalyst layer can be forced to undergo corrosion, which generates carbon dioxide (CO_2) at the cathode. Although the O_2 is not used at the cathode under ADT tests, the combination of H_2O supplied in the humidified N_2 with the carbon support of the catalyst can react to produce CO_2 under high voltage conditions [26]. According to the mechanism of carbon corrosion reported in Ref. [26], the functional oxygen groups ($C{-}O_{ad}$) are generated on the carbon surface and are then

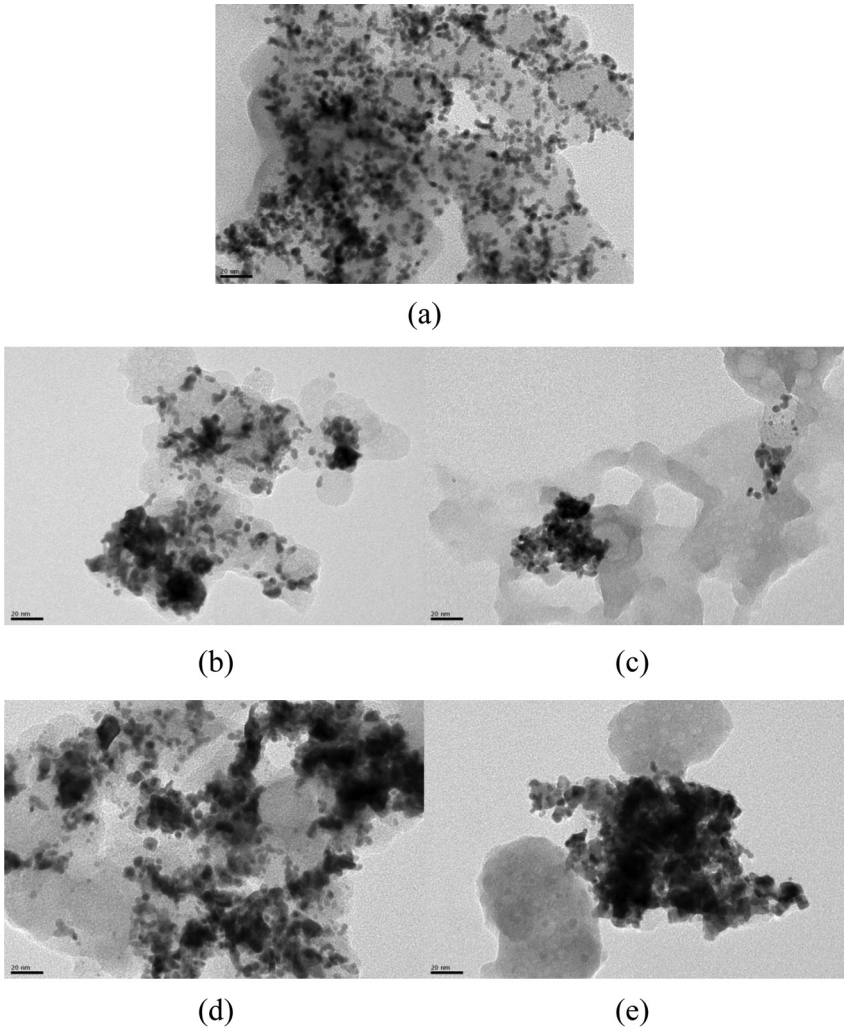

Fig. 6. TEM image of the catalyst layer. (a) Initial (t = 0 min), (b) ADT 30 min (anode side), (c) ADT 150 min (anode side), (d) ADT 30 min (cathode side), and (e) ADT 150 min (cathode side).

converted into CO_2. In the present study, a real-time gas analyzer (RTGA) at the cathode exit for the ADT duration (0–150 min) was used to measure the generated CO_2 due to the carbon corrosion. In Fig. 5, the horizontal axis represents the ADT testing time and the vertical axis represents the ion intensity. Observation of a greater ion intensity indicates a faster gas formation rate (CO_2) at the cathode. The RTGA was purged with N_2 for an hour prior to initiating the ADT testing to allow the apparatus to distinguish the released gases with greater certainty in the measurement. Fig. 5 clearly indicates that the CO_2 was detected as soon as the ADT testing began. The detected CO_2 levels peaked at 20 min during the ADT testing, similar to the peak described in Ref. [26] at 10–20 min, after which they slowly decreased to reach a plateau at approximately 60 min. The spike towards 0 indicates that no CO_2 is detected at specific moments after 5 min.

Recently, Jung and his coworkers [26] reported that the aging mechanism for MEAs of low-temperature PEM fuel cells under ADT testing is due to the corrosion of the carbon support, which may also cause the dissolution or agglomeration of the platinum in the catalyst. To confirm this mechanism, sections of the catalyst layers at both the anode and the cathode were scraped off after each ADT testing stage. The samples were then analyzed by TEM imaging to determine the changes in the microstructures of the samples. The catalyst microstructures at the anode and the cathode before and after ADT testing are depicted in Fig. 6. The catalyst microstructure prior to the ADT test (initial) indicated uniform adhesion between the platinum and carbon support. After 30 min of ADT testing, the platinum became localized near the edges of the carbon support, which indicates the corrosion of the surroundings of the carbon support. In addition, the platinum concentration decreased considerably compared to that before ADT testing. This decreased concentration indicates that dissolution and accumulation of the platinum occurred in the catalyst during ADT test, thus causing a reduction of the reaction area. With the increase in the ADT time, the agglomeration of platinum around the carbon support became significant. This agglomeration causes a decline in the reaction area, corresponding to a decrease in the electrochemical reaction area and the cell performance. At 150 min of ADT testing, the carbon support was seriously corroded, with only a few Pt catalyst clusters remaining adhered. Therefore, a seriously degraded cell performance was noted for a longer ADT testing (ADT 150 min), as shown in Fig. 2. While the both anode and cathode catalyst layer exhibited a similar change, the extent of this change was significantly lower in the anode catalyst layer. Although Pt within anode catalyst experiences lower potential with less carbon corrosion, Pt nanoparticles remain unstable and agglomerate to large particles. In addition to self-agglomeration of Pt nanoparticles, the carbon corrosion within the cathode catalyst layer of the HT-PEM fuel cell is one of the main reasons for the observed cell performance reduction and could result in further relocation and agglomeration of platinum in the catalyst layer, which in turn, causes the decline in the cell performance of fuel cell.

4. Conclusions

In this work, the performance degradation of a high-temperature PEM fuel cell was examined by an accelerated degradation technique (ADT) with 30 min intervals. The characterization of the MEAs was performed using in-situ and ex-situ electrochemical methods, such as polarization curves, AC impedance, cyclic voltammetry (CV), and TEM imaging before and after the ADT experiments. The conclusions we have drawn from the measured results are as follows:

(1)The measured results indicate that the ADT testing could dramatically reduce the duration of the degradation. Current output at 0.4 V decreased by 48% after performing ADT testing for 30 min.

(2)The cathode polarization losses (R_c, low frequency) at various stages of the ADT testing were increased with the ADT times, which led to a decrease in the cell performance. With the increase of the current densities, the charge transfer resistances decreased, due to the greater driving force.

(3)From the AC impedance, LSV, CV and RTGA measurements, the decline in cell performance was found to be primarily due to corrosion and thinning of the cathode catalyst layer (or carbon support) during the ADT testing, leading to further dissolution and agglomeration of the platinum catalyst.

Acknowledgments

The authors acknowledge the Energy Bureau and National Science Council of Taiwan under contracts 101-2622-E-155-004-CC2, 100-2221-E-155-082-MY2, 102-2221-E-155-005-MY3, and 102-2622-E-155-001-CC2, for providing the financial support.

References

[1] J.T. Wang, R.F. Savinell, J. Wainright, M. Litt, H. Yu, Electrochim. Acta 41 (1996) 193.
[2] J. Zhang, Z. Xie, J. Zhang, Y. Tang, C. Song, T. Navessin, J. Power Sources 160 (2006) 872.
[3] J.O. Jensen, Q. Li, C. Pan, A.P. Vestbo, K. Mortensen, H.N. Petersen, Int. J. Hydrogen Energy 32 (2007) 1567.
[4] A.R. Korsgaard, R. Refshauge, M.P. Nielsen, M. Bang, S.K. Kaer, J. Power Sources 162 (2006) 239.
[5] R.H. He, Q.F. Li, G. Xiao, N.J. Bjerrum, J. Membr. Sci. 226 (2003) 169.
[6] Q. Li, C. Pan, J.O. Jensen, P. Noyé, N.J. Bjerrum, Mater. Chem. 19 (2007) 350.
[7] P. Staiti, M. Minutoli, J. Power Sources 94 (2001) 9.
[8] P. Staiti, M. Minutoli, S. Hocevar, J. Power Sources 90 (2000) 231.
[9] A.L. Ong, G.B. Jung, C.H. Wu, W.M. Yan, Int. J. Hydrogen Energy 35 (2010) 7866.
[10] N.H. Jalani, M. Ramani, K. Ohlsson, S. Buelte, G. Pacifico, R. Pollard, J. Power Sources 160 (2006) 1096.
[11] J. Zhang, Y. Tang, C. Song, J. Zhang, J. Power Sources 172 (2007) 163.
[12] Y. Oono, T. Fukuda, A. Sounai, M. Hori, J. Power Sources 195 (2010) 1007.
[13] S. Galbiati, A. Baricci, A. Casalegno, R. Marchesi, Int. J. Hydrogen Energy 37 (2012) 2462.
[14] T.J. Schmidt, J. Baurmeister, ECS Trans. 3 (2006) 861.
[15] L.A. Diaz, G.C. Abuin, H.R. Corti, J. Power Sources 188 (2009) 45.
[16] J. Hu, H. Zhang, Y. Zhai, G. Liu, B. Yi, Int. J. Hydrogen Energy 31 (2006) 1855.
[17] H.L. Lin, Y.S. Hsieh, C.W. Chiu, T.L. Yu, L.C. Chen, J. Power Sources 193 (2009) 170.
[18] Y. Oonoa, A. Sounaib, M. Horia, J. Power Sources 210 (2012) 366.
[19] G. Liu, H. Zhang, J. Hu, Y. Zhai, D. Xu, Z. Shao, J. Power Sources 162 (2006) 547.
[20] J.W. Hu, H.M. Zhang, Y.F. Zhai, G. Liu, J. Hua, B.L. Yi, Electrochim. Acta 52 (2006) 394.
[21] A.D. Modestov, M.R. Tarasevich, V.Y. Filimonov, N.M. Zagudaeva, Electrochim. Acta 54 (2009) 7121.
[22] S. Yu, L. Xiao, B.C. Benicewicz, Fuel Cells 8 (2008) 165.
[23] T.J. Schmidt, J. Baurmeister, J. Power Sources 176 (2008) 428.
[24] T.C. Jao, S.T. Ke, P.H. Chi, G.B. Jung, S.H. Chan, Int. J. Hydrogen Energy 35 (2010).
[25] T.C. Jao, G.B. Jung, P.H. Chi, S.T. Ke, S.H. Chan, J. Power Sources 196 (2011) 1818.
[26] G.B. Jung, K.Y. Chuang, T.C. Jao, C.C. Yeh, C.Y. Lin, Appl. Energy 100 (2012) 81, 6941.
[27] H. Katie, H.S. Lim, S.E. Oh, Y.J. Jang, H.J. Ko, H.K. Kim, J. Power Sources 193 (2009) 575.
[28] H.S. Oh, J.G. Oh, S. Haam, K. Arunabha, B. Roh, I. Hwang, Electrochem. Commun. 10 (2008) 1048.
[29] Q. Shen, M. Hou, D. Liang, Z. Zhou, X.J. Li, Z. Shoo, J. Power Sources 189 (2009) 1114.
[30] J.P. Meyers, R.M. Darling, J. Electrochem. Soc. 153 (2006) A1432.
[31] H. Tang, Z. Qi, M. Ramani, J.F. Elter, J. Power Sources 158 (2006) 1306.
[32] R.A. Silva, T. Hashimoto, G.E. Thompson, C.M. Range, Int. J. Hydrogen Energy 37 (2012) 7299.
[33] R. O'Hayre, S.W. Cha, W. Colella, F.B. Prinz, Fuel Cell Fundamentals, second ed., Wiley & Sons, 2009, p. 248.